

HOSTED BY



Contents lists available at ScienceDirect

Journal of King Saud University – Science

journal homepage: www.sciencedirect.com



Original article

Biomimetic formation of silver oxide nanoparticles through *Diospyros montana* bark extract: Its application in dye degradation, antibacterial and anticancer effect in human hepatocellular carcinoma cells



Venugopal Sujatha^{a,b,*}, Gunaseelan Kaviyasri^a, Alagesan Venkatesan^a, Chinnasamy Thirunavukkarasu^c, Sancharan Acharya^c, Salman Bin Dayel^d, Sameer Al-Ghamdi^e, Mohammad Hassan Abdelzaher^{f,g}, Mohammad Shahid^f, Thiyagarajan Ramesh^f

^a DST-Mobility Fellow, Department of Chemistry, Pondicherry University, Puducherry 605 014, India

^b Department of Chemistry, Periyar University, Salem 636 011, TN, India

^c Department of Biochemistry and Molecular Biology, Pondicherry University, Puducherry 605 014, India

^d Dermatology Unit, Internal Medicine Department, College of Medicine, Prince Sattam Bin Abdulaziz University, Al-Kharj 11942, Saudi Arabia

^e Family and Community Medicine Department, College of Medicine, Prince Sattam Bin Abdulaziz University, Al-Kharj 11942, Saudi Arabia

^f Department of Basic Medical Sciences, College of Medicine, Prince Sattam Bin Abdulaziz University, Al-Kharj 11942, Saudi Arabia

^g Department of Medical Biochemistry, Faculty of Medicine, Al-Azhar University, Assiut branch, Egypt

ARTICLE INFO

Article history:

Received 27 November 2022

Revised 15 December 2022

Accepted 10 January 2023

Available online 16 January 2023

Keywords:

Mitochondrial membrane potential

DNA damage

Autophagy

ABSTRACT

Objectives: Remarkable potential of silver nanoparticles (NPs) makes its use efficient in both biological as well as industrial applications. Post harvested NPs, free from other hazardous chemicals will be ideal for biological applications. Thus, plant mediated biological method is much focused than the available approaches.

Methods: The present work focusses on fabrication of silver oxide NPs (Ag₂ONPs) using methanolic bark extract of *Diospyros montana* and characterized through sophisticated analytical techniques.

Results: UV–Vis indicated Ag₂ONPs formation, FTIR analysis identified the functional groups, XRD investigation depicted the face centered cubic crystalline nature, XPS study determined the chemical state, EDX confirmed the purity, spherical shaped and ~ 10–50 nm size, was evidenced by SEM and TEM respectively. Zeta potential denoted the stability of Ag₂ONPs. Photocatalytic degradation of methylene blue was observed. Ag₂ONPs showed significant anticancer effect against hepatocellular carcinoma cells (Hep G2), which is mediated through increased DNA damage, & autophagy and decreased mitochondrial membrane potential. The synthesized Ag₂ONPs revealed significant zone of inhibition in gram-negative (*Escherichia coli* – 16.33 ± 2.57 and *Pseudomonas aeruginosa*–18.56 ± 1.57) and positive (*Bacillus subtilis*–22.26 ± 4.47, *Staphylococcus aureus* 18.65 ± 3.15) bacteria at 40 µg/mL of Ag₂ONPs exhibiting its antibacterial property.

Conclusions: This enlightens the synthesis of pure and stable Ag₂ONPs by green synthesis unwrapping their pharmacological properties which may play a vital role in nanomedicine anchoring its therapeutic efficiency.

© 2023 The Author(s). Published by Elsevier B.V. on behalf of King Saud University. This is an open access article under the CC BY-NC-ND license (<http://creativecommons.org/licenses/by-nc-nd/4.0/>).

1. Introduction

Nanoparticles (NPs) have immensely attracted the scientific community because of its high reactivity due to ratio of high surface area to volume with eminent properties. Green synthesis technology by plants is economical, eco-friendly, sustainable, rapid and biocompatible (Singh et al. 2018; Palanisamy et al. 2017). Reports reveal the versatile pharmacological properties of the phytoconstituents present in the plants (Kathirvel and Sujatha, 2016.) Green synthesis of nanoparticles serves as a beneficial method among the

* Corresponding author.

E-mail addresses: sujathav.che@pondiuni.edu.in, sujatha888@periyaruniversity.ac.in (V. Sujatha).

Peer review under responsibility of King Saud University.



Production and hosting by Elsevier

<https://doi.org/10.1016/j.jksus.2023.102563>

1018–3647/© 2023 The Author(s). Published by Elsevier B.V. on behalf of King Saud University.

This is an open access article under the CC BY-NC-ND license (<http://creativecommons.org/licenses/by-nc-nd/4.0/>).

other available methods (Das et al. 2017). Based on their easy availability and efficient synthesis, eco-friendly green synthesis serves as a value-added technology in synthesizing metal oxide NPs thereby serving a vital role in the field of nanomedicine (Devanesan and AlSalhi, 2021). Research on nanoparticle synthesis using medicinal plants has gained immense attraction of the scientists based on their efficient synthesis and versatile biological applications.

A medicinally important plant, *Diospyros montana* (*D. montana*) (F: Ebenaceae), the Bombay Ebony, is a small deciduous tree, of 15 m height, found widely in Sri Lanka, Western Ghats of India and Indo-China. We have reviewed the occurrence of various biomolecules namely, phenols, carbohydrates, flavonoids, tannins, anthocyanins followed by anthraquinones (Sujatha and Venkatesan, 2022). Literature reveals the presence of various chemical constituents in the roots (Khan et al. 2020). We have reported that leaf extract of *D. montana* contains various bioactive principles and also observed that this extract could make an efficient synthesis of selenium NPs (Kokila et al. 2017). It has also extended its potential in biological applications. This interesting finding made us to analyse the other parts of the plant such as bark. Further, we also studied the pharmacological applications of green synthesis of silver oxide NPs (Ag_2ONPs) to explore its beneficial pharmacological properties. Metal oxide NPs possess potential applications based on their unique optical, electronic, magnetic and other physico-chemical characteristics (Mao et al. 2005). Metal-oxide NPs has dragged the researchers based on their multi-faceted properties and therapeutic efficacy. Among the NPs, Ag_2ONPs possess versatile biomedical applications (Aisida et al. 2021). It also has other significant pharmacological applications namely anti-inflammatory, anticancer and antibacterial effects (Aisida et al. 2021; Lekshmi et al. 2022).

UV-vis spectroscopy (UV-Vis) and Fourier transform infrared (FTIR) were used to identify the formation of NPs. X-ray powder diffraction (XRD) and X-ray photoelectron spectroscopy (XPS) were adopted to examine chemical composition. Energy dispersive X-ray analysis (EDX), scanning electron microscopy (SEM), and transmission electron microscopy (TEM) techniques were used to study the purity, morphology, and topology. Dynamic light scattering (DLS) and zeta potential have been studied to analyse the stability of the phyto-mediated Ag_2ONPs synthesized. The dye degradation effect of Ag_2ONPs has been studied through methylene blue (MB). *In vitro* anticancer and antibacterial studies were performed to evaluate its pharmacological applications. The aim of the current investigation focusses on the biological creation of Ag_2ONPs through the methanol bark extract (MeBEs) of *D. montana*, and its biological applications, which is first of its kind.

2. Experimental

2.1. Chemicals used

Silver nitrate (AgNO_3) (99% purity) was procured from Sigma-Aldrich Chemical, India. From Himedia, 3-(4,5-dimethylthiazol-2-yl)-2,5-diphenyl tetrazolium bromide (MTT), 5,5,6,6'-tetrachloro-1,1',3,3' tetraethylbenzimidazolylcarbocyanine iodide (JC-1), 4',6'-diamidino-2-phenylindole (DAPI), acridine orange (AO), 10x phosphate buffered saline (PBS), dimethyl sulfoxide (DMSO), fetal bovine serum (FBS), and Dulbecco's modified Eagle's medium (DMEM) were obtained. From National Centre for Cell Science (NCCS), Pune, India HepG2 cells were procured. All other required reagents (analytical grade and > 95% pure) were obtained from Merck India Private Limited and Himedia companies.

2.2. Plant collection

D. montana was obtained between the month of October to November, from Krishnagiri District Hills, recognized and confirmed by Botanical Survey of India, [BSI/SRC/21/11/2019/Tech/1791](Kokila et al. 2017), Coimbatore, TN, India. MeBEs was obtained by Soxhlet extraction equipped with 200 g of bark sample and added methanol of 300 mL followed by 72 hrs continuous running. The extracted sample was filtered, dried and used for further study.

2.3. Preliminary phytochemical and quantification of phenol and flavonoid

Standard qualitative methods were adopted to examine the various phytochemical occurrences (Onwukeame, et al. 2007). The total phenol and flavonoid contents available in the MeBEs were quantified by colorimetric method (Barreira et al. 2008).

2.4. Phyto-mediated synthesis of Ag_2ONPs

Deionized water was used to prepare 1 mM, AgNO_3 solution. 10 mL of 10% (w/v) MeBEs was added drop-by drop to 90 mL of 1 mM AgNO_3 , with continuous stirring. The composition was stirred continuously at 90 °C for 3 h. Initial identification of Ag_2ONPs production was inferred by the brownish black color of the solution. The black precipitate formed was washed with ethanol thrice and separated by centrifuging at 1000 rpm for 30 min. The precipitate was allowed to dry at room temperature (25 °C) overnight to obtain its powder form. The fine powdered sample of Ag_2ONPs was stored in air tight bottle for future analysis.

2.5. Ag_2ONPs characterization

The absorption maxima of Ag_2ONPs were identified by double-beam spectrophotometer ranging from 200 to 800 nm at a scanning speed of 480 nm/min. Perkin-Elmer UV-Vis spectrophotometer (Waltham, MA, USA) equipped with "UV Winlab" software. FTIR spectroscopy (Thermo Nicolet 6700) was used to examine the functional groups of Ag_2ONPs . The grain size and phase purity of Ag_2ONPs was analysed using Rigaku ultima IV XRD. Debye-Scherrer formula $D = 0.9 \lambda / \beta \cos \theta$ was adopted to calculate the average particle size (D). The oxidation state of the nanoparticle was recorded by XPS (Thermo Scientific K α -KAN9954133). Chemical composition and purity of the Ag_2ONPs was analysed by electron microscope FESEM-EDX Carl Zeiss Sigma 300 VP (Carl Zeiss Microscopy GmbH (Jena, Germany). Morphology of the NPs was exhibited by SEM (Jeol 6390LA). TEM was visualized and documented using JEOL/ JEM 2100 equipped with electron diffraction pattern. Average size and stability of the NPs was examined by DLS and zeta potential (Malvern, Zeta Sizer Nano S, USA).

2.6. Dye degradation determination of Ag_2ONPs :

The dye degradation property of Ag_2ONPs was examined with MB (Kadam et al. 2020). The Ag_2ONPs + MB was exposed to bright sunlight and absorbance spectra was recorded at every 2 h interval up to 6 h until the MB color faded visually and recorded using UV-Vis.

2.7. Biological applications assessment

Through MTT assay the anticancer effect of Ag₂ONPs was performed against HepG2 liver cancer cells as explained in Subastri et al. (2018).

Nuclear morphology and autophagy: Double-stranded (ds) and single-stranded (ss) nucleic acids are differentiated through staining by a metachromatic dye such as AO. Excitation at 480–490 nm emits green fluorescence upon AO intercalates into dsDNA. On the other hand, when, AO interacts with ssDNA or RNA emits red color. Acidic vesicular organelles (AVO) such as autolysosomes accumulates in it the protonated form of fluorophore namely AO (Thomé et al., 2016).

Mitochondrial membrane potential (MMP) was examined through JC-1 staining (Perelman et al., 2012). The HepG2 cells were treated with Ag₂ONPs 24 h at 37 °C, subsequently cells were incubated with JC-1 stain (1 µg/mL) with the nuclear stain DAPI (1 µg/mL) for 30 min at 37 °C. After experimental period, the cells were thoroughly cleaned with 1 × PBS, MMP was examined under the fluorescence microscope Olympus CX 40, USA. Further, fluorescence strength was estimated through Image J software.

Antibacterial property of the Ag₂ONPs against *Bacillus subtilis* & *Staphylococcus aureus* (gram-positive) and *Escherichia coli* & *Pseudomonas aeruginosa* (gram-negative) was evaluated by agar diffusion method as explained by Srinivasan et al. (2016).

2.8. Statistical analysis

SPSS software (version 16.0) was used for statistical analysis. Comparison of significant differences between samples with 95% confidence limits at $p < 0.05$ was done by Tukey's multiple range tests.

3. Results and discussion

Green synthesized NPs are more preferred than that of the other methods, when aimed for pharmacological applications. Phytochemical screening provides the vast identification of the phytoconstituents available in the medicinal plant which may be accountable for its significant properties and applications. Phytochemical screening analysis of *D. montana* MeBEs, exposed the existence of bio constituents viz., flavonoids, tannins, steroids, terpenoids, alkaloids, carbohydrates and phenolics. (Table S1). Flavonoids, phenols, alkaloids, tannins, carbohydrate and proteins were intensely present. Terpenoids, steroids, saponins and fats were found to be moderately present. Presence of various phytoconstituents made us to evaluate its antioxidant property of this extract.

3.1. Antioxidant contents

The MeBEs of *D. montana* contained 28.45 ± 4.63 µg of catechin equivalents/mg of extract of flavonoids and 41.58 ± 5.41 µg of gallic acid equivalents/mg of extract of phenolic contents (Table S2). Our previous report in the leaf extract of *D. montana* also showed the occurrence of flavonoid and phenolic contents. (Kokila et al. 2017). The present and previous findings indicate that both leaf and bark of *D. montana* could be a good source of different flavonoids and phenolic compounds. Tannins serve as the natural reducing agent by their hydroxyl groups present in them which reduces metallic ions (Raja et al. 2014). Mathew et al. (2015) reported the role of phenolic compounds as redox agents and oxygen quenchers depends on its phenolic hydroxyl groups which possess redox properties. Medicinal plants composed of significant

phytoconstituents are stated to serve as bio-reductants of metallic ions in aqueous condition. The phytoconstituents, serve as an efficient natural resource of reducing and capping molecules thereby facilitating the formation of NPs (Kokila et al. 2017). The presence of various phytoconstituents in MeBEs observed in the present findings, may help in efficient synthesis of NPs. Therefore, we made an attempt to test its efficacy in AgNO₃ as metal precursor to synthesize Ag₂ONPs.

3.2. Green synthesis and characterization of Ag₂ONPs

Ag₂ONPs was synthesized from the metal precursor, AgNO₃. Brownish black color was observed denoting the formation of Ag₂ONPs (Fig. 1A). This efficient synthesis may be due to the presence of other potent phytoconstituents namely tannins, alkaloids, steroids and saponins present in the MeBEs. Tannins are reported to serve as natural reducing agent (Raja et al. 2014). The formation of green synthesized Ag₂ONPs was indicated through UV–Vis analysis (Fig. 1B and C). The MeBEs of *D. montana* showed the peak at 362 nm corresponding to the $\pi \rightarrow \pi^*$ transition, indicating the characteristic of flavonoid and phenolic substances occurring in the extract (Fig. 1B). The UV–Vis spectra exhibited the strong surface plasmon resonance (SPR) peak at 405 nm authorizing the complete development of Ag₂ONPs (Fig. 1C). The flavonoid and phenolic phytoconstituents of the plant extract containing the hydroxy and ketonic groups may be responsible in reducing the bulk metal silver to its nano form (Manikandan et al. 2017). Fig. 1C portrays the outcome of reaction period on the UV–vis spectra of synthesized Ag₂ONPs. It is evident that the strength of the absorbance peak increases linearly with growing time of the reaction with an interval of 5 min up to 30 min. This could be due to the rapid production of Ag₂ONPs by the reduction of silver ions existing in the aqueous medium (Wei et al. 2020). Results observed in the current investigation are in line with previous investigations (Okafar et al. 2013; Velsankar et al. 2022).

The FTIR spectrum displays the functional moieties of various phytochemicals existing in the MeBEs (Fig. 2A) and Ag₂ONPs (Fig. 2B). The peaks at 3424, 2935, 1728, 1611, 1443, 1327, 1185, 1037, 735 cm⁻¹ in the MeBEs of *D. montana* was shifted to 3692, 3011, 2888, 2360, 1717, 1378, 849 cm⁻¹ indicating the development of Ag₂ONPs. The *D. montana* MeBEs showing a wide band at 3424 cm⁻¹ corresponds to O–H stretching assigned to alcohols. The C–H stretching (alkanes) was observed as doublet at 2935 and 1443 cm⁻¹ and C–O stretching was observed as triplet at 1728, 1185 and 1037 cm⁻¹ to alcohols. The intense band observed at 1611, 1327 and 735 cm⁻¹ is characteristic nature of N–H, C–N stretching (amines) and C–H out of plane bending (alkenes) modes. The Ag₂ONPs revealed broad peak at 3692 cm⁻¹ reveals the occurrence of alcohols (O–H stretching). The aromatic C–H stretching was observed as doublet at 3011 and 2888 cm⁻¹. The bands attributed at 2360, 1717 and 1378 cm⁻¹ is characteristic nature of C–N, C–O and C–N stretching modes. The frequency peak at 849 cm⁻¹ attributes to the structural vibration which conform the existence of metal oxide stretching mode. The FTIR analysis infers the function of phytoconstituents as stabilizers and capping substances in the formation of NPs and further may be contributing the reduction of Ag⁺ to Ag⁰ (Manikandan et al. 2017).

The XRD outline of Ag₂ONPs manufactured through MeBEs of *D. montana* is depicted in Fig. 2C. Diffraction peaks at $2\theta = 38.22^\circ$, 44.28° , 64.49° , and 77.54° parallels to (111), (200), (220), and (311) planes of Ag₂ONPs which corresponds to characteristic face centered cubic structure (Roy et al. 2015). The strong and narrow thin peaks indicate the crystalline phase of the synthesized NPs. These diffraction patterns are in finest resemblance with the JCPDS No. 04–0783 and are well crystalline (Manikandan et al. 2017). The strong strength of diffraction at 38° denotes silver crystal's at

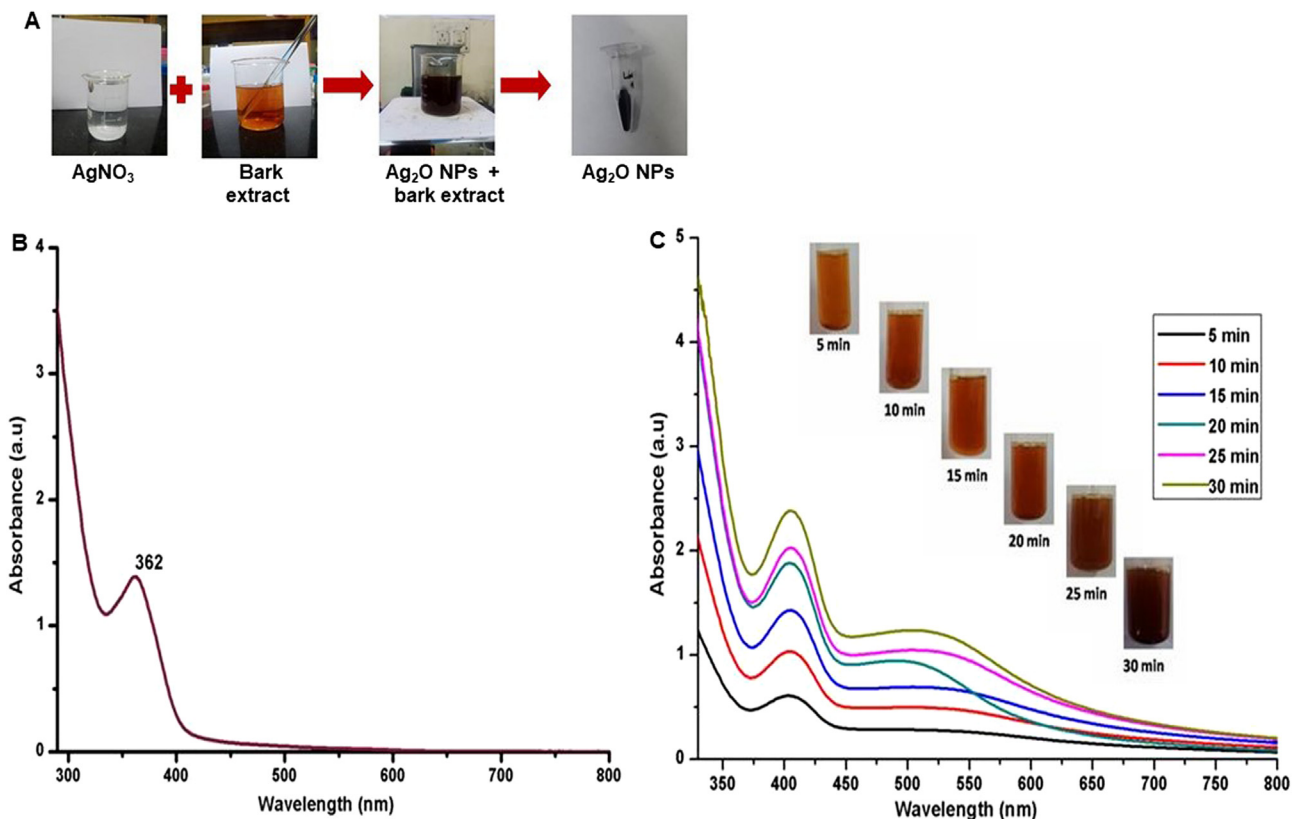


Fig. 1. (A) Synthesis of Ag₂ONPs (B) UV-Vis absorption of bark extract and (C) UV-Vis absorption of Ag₂ONPs.

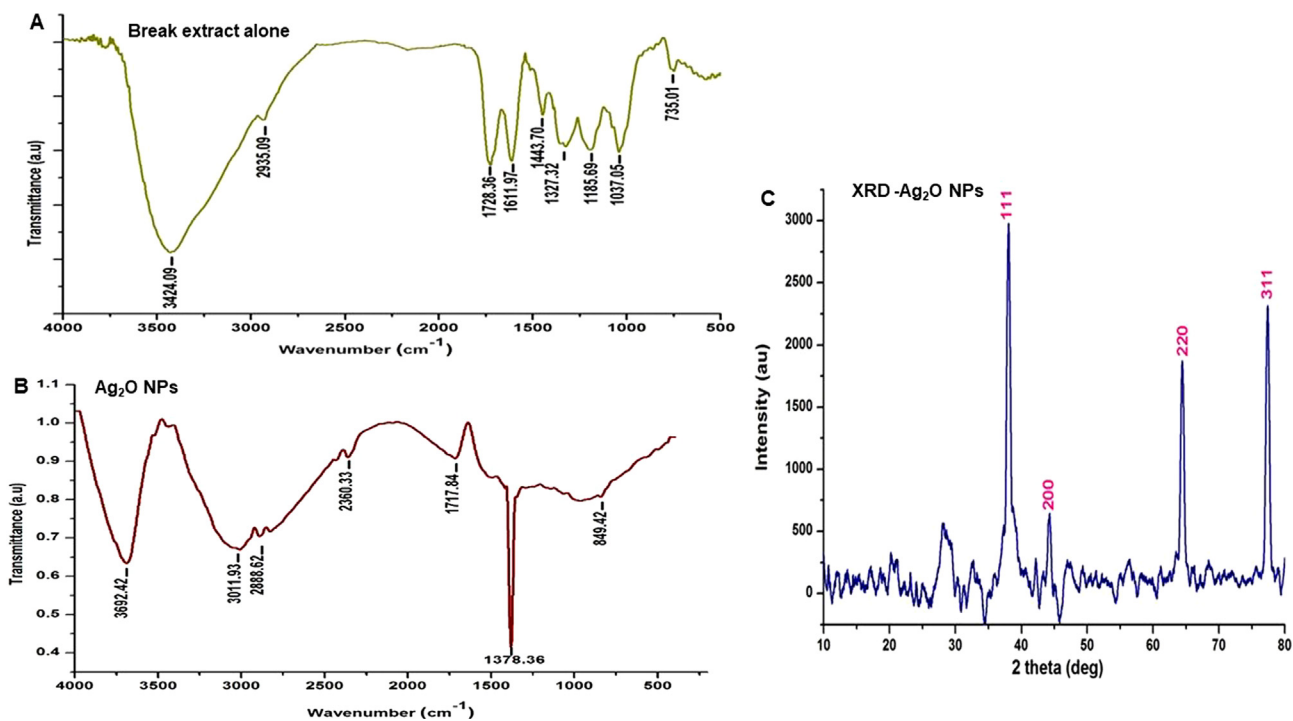


Fig. 2. Shows FTIR and XRD spectra - (2A) FTIR of bark extract, (2B) FTIR of Ag₂ONPs and (2C) XRD.

avored positioning along (111) plane. The average particle size of the Ag₂O NPs was observed to be 21.3 nm calculated through Debye-Scherrer's formula.

Fig. S1 portrays the XPS spectra of Ag₂ONPs. Fig. S1A shows high-resolution peak of Ag 3d and O of the synthesized Ag₂ONPs. Fig. S1B shows the orbits of 3d_{5/2} and 3d_{3/2} exhibiting the binding

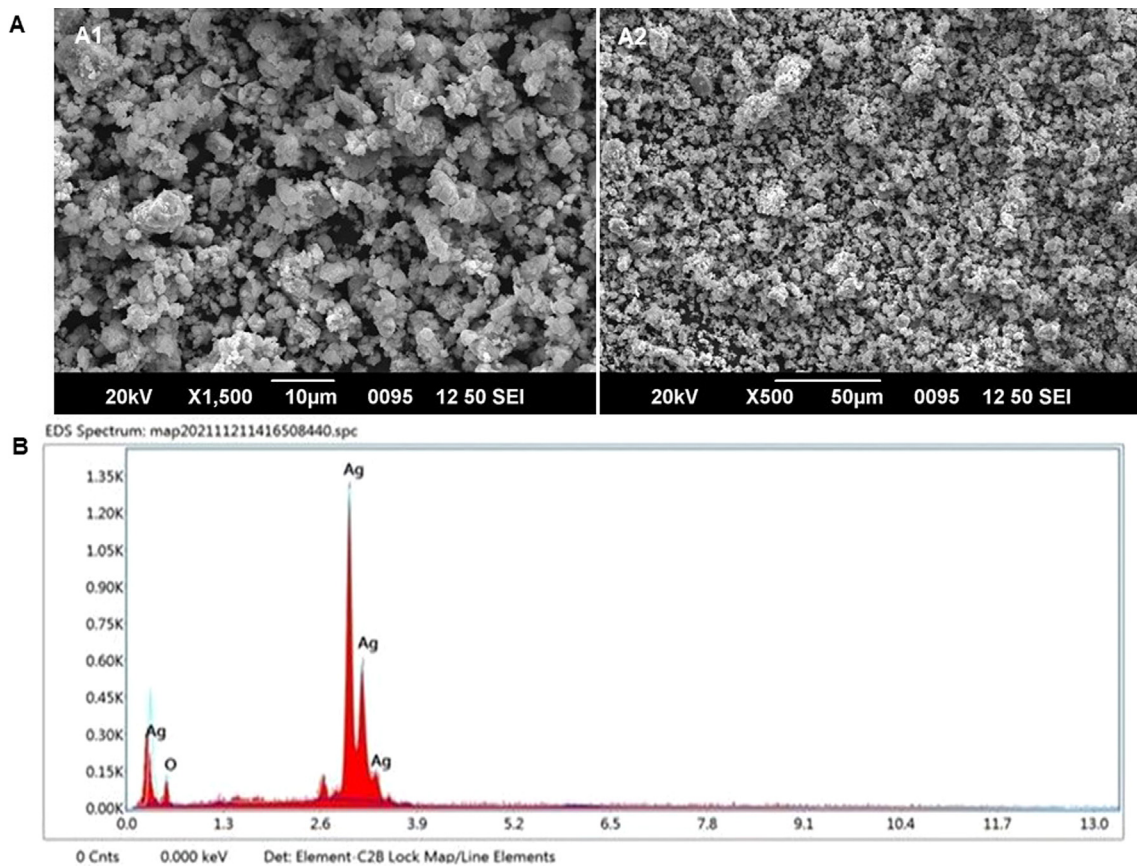


Fig. 3. Ag₂ONPs – (A1) SEM image at 10 μm (A2) at 10 μm and (B) EDX mapping.

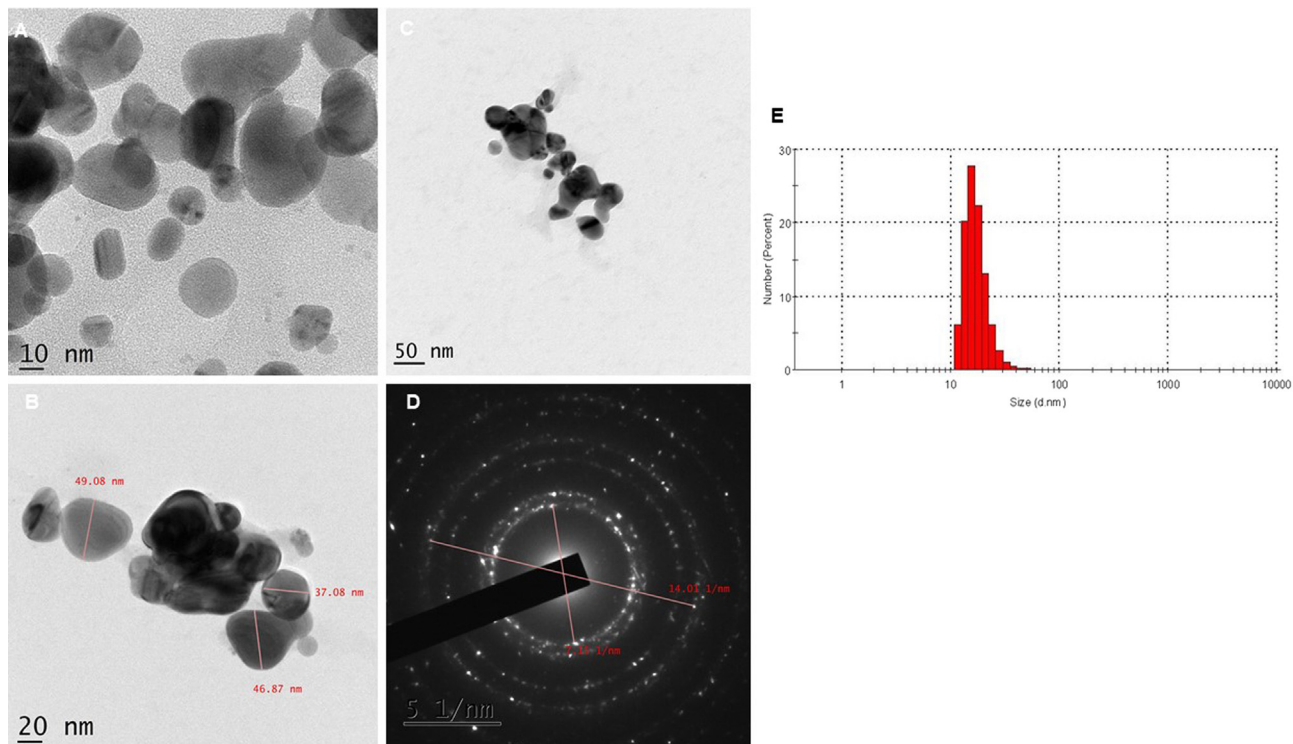


Fig. 4. Pictures depicts TEM images of Ag₂ONPs. Fig. 4(A) 10 nm, (4B) 20 nm, (4C) 50 nm magnification and (4D) SAED pattern and (5E) DLS.

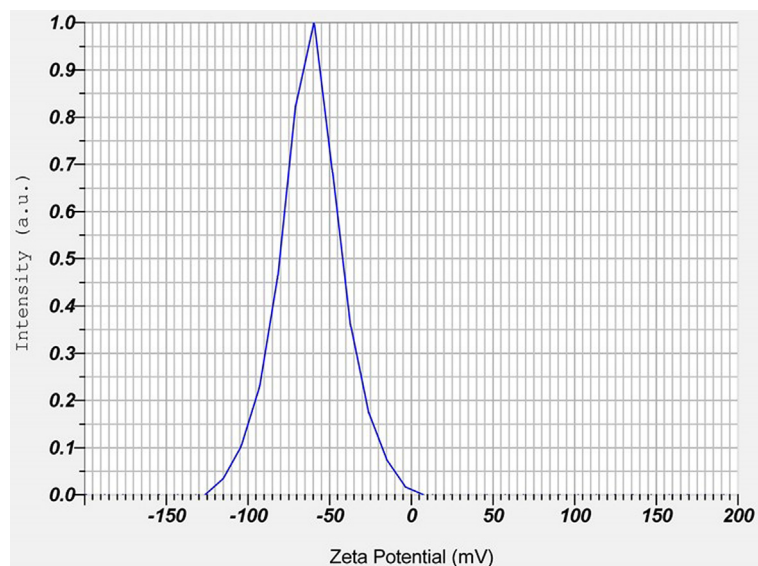


Fig. 5. Zeta potential of Ag₂ONPs.

energy peak of metallic silver at 368.5 eV and 374.6 eV correspondingly. (Ajitha et al. 2015). Fig. S1C exhibits the presence of oxygen at 532.7 eV corresponding to the 1 s orbit of oxygen in the high-resolution spectrum obtained. This authenticates the synthesis of B-Ag₂ONPs. Fig. S1D displays the orbit C 1 s corresponding to the carbon peak observed at 284.8 eV. In addition, no extra peaks were observed in the XPS spectra signifying the synthesized Ag₂ONPs are free of impurities (Maheshwaran et al. 2020). The current observation coincides with the findings of Velsankar et al. (2022).

SEM analysis exhibited the shape of the synthesized Ag₂ONPs (Fig. 3A). Spherical shaped Ag₂ONPs was evidenced by SEM analysis (Fig. 3A1). Further, picture depicts that the particles are dispersed non-uniformly with a smooth and perfect morphology (Fig. 3A2). The NPs formed are spherical in shape and agglomerated as evidenced by Devanesan and ALSalhi, (2021). This agglomeration may be owed to the polarity and electrostatic affinity of the NPs. The results are well correlated with earlier literature (Aiswariya and Jose, 2022). Fig. 4B depicts the EDX spectrum of the synthesized Ag₂ONPs, which are free of impurities along with the atomic and weight percentages of silver and oxygen which denotes the development of pure Ag₂ONPs. The compositions of O and Ag were observed as 10.11, 89.89 (weight %) and 43.12, 56.88 (atomic %) respectively. As elemental nitrogen is absent it confirms the reduction of AgNO₃ to Ag₂ONPs. Existence of metallic silver is indicated by the occurrence of intense band and sharp peak at 3 keV which is the characteristic of it (Aiswariya and Jose, 2022). The weight percentage and impurities free phyto-mediated Ag₂ONPs are established through EDX spectrum. TEM images (Fig. 4 A-C) exhibited the spherical form of the NPs in various magnifications supporting the SEM images. NPs were obtained in size ranging from ~ 6 nm to ~ 50 nm as shown in the pictures. The bright circular spots in the SAED pattern (Fig. 4D) confirms the crystalline form of the NPs as evidenced by XRD analysis. Nanoparticle shape, size, surface properties, route of administration and dispersion medium are some of the vital parameters responsible for their biological property which includes therapeutics and toxicity. DLS estimates the average size and distribution of the Ag₂ONPs dispersed in liquid (Fig. 4E). The average size of the Ag₂ONPs was found to be in the range of 11.7–58.77 nm. In the current study, smaller size NPs are formed, as evidenced through the DLS with lower range of particle size. Our results are also supported by Ahmed et al. (2016).

Zeta potential analysis was examined to study the stability of the NPs (Fig. 5). It showed the intense stability of the NPs. The zeta potential around the surface of the particles was recorded as –61.4 mV, indicating the excellent stability of the NPs. In the present investigation, we have observed negative charge on the surface of the Ag₂ONPs, which depicts its charge. The findings indicate that the synthesized Ag₂ONPs can preserve their structure for long-term (Erdogan et al. 2019). Nanoparticle stability shall evidence the preservation of nanostructure reflecting its properties based on shape and size of the nanoparticle. Reports reveal that NPs produced from plants are found to be more stable (Sadeghi and Gholamhoseinpoor, 2015). The green synthesized silver NPs are found to be of higher stability and well-correlated with other reports.

3.3. Applications of Ag₂ONPs

Fig. 6 shows the photocatalytic property of the Ag₂ONPs. Existing methods such as, chemical oxidation, membrane filtration etc

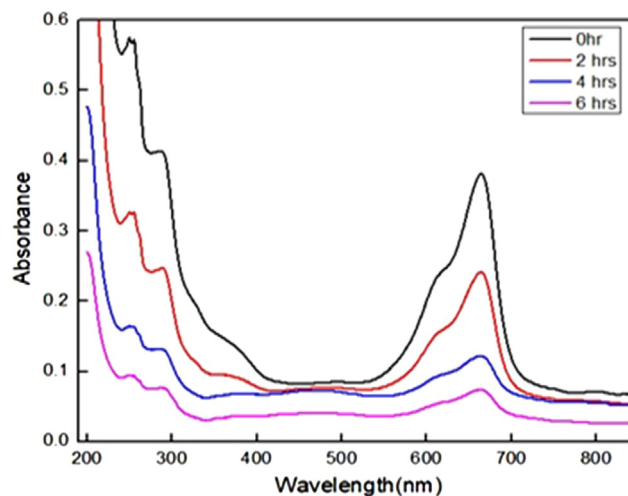


Fig. 6. Photocatalytic property of Ag₂ONPs.

involved in dye removal has one or other restrictions (Dizge et al. 2008). Metal NPs are widely used for the degradation of the coloured waste based on its efficient role (Kale and Kane, 2017). Photocatalytic degradation activity of Ag₂ONPs was carried out

with MB under natural sunlight. The dye degradation was noticed visually through the gradual colour discharge from blue to light green. Absorption peak observed at 665 nm was found to be decreased with increase in time. The excitation of surface plasmon

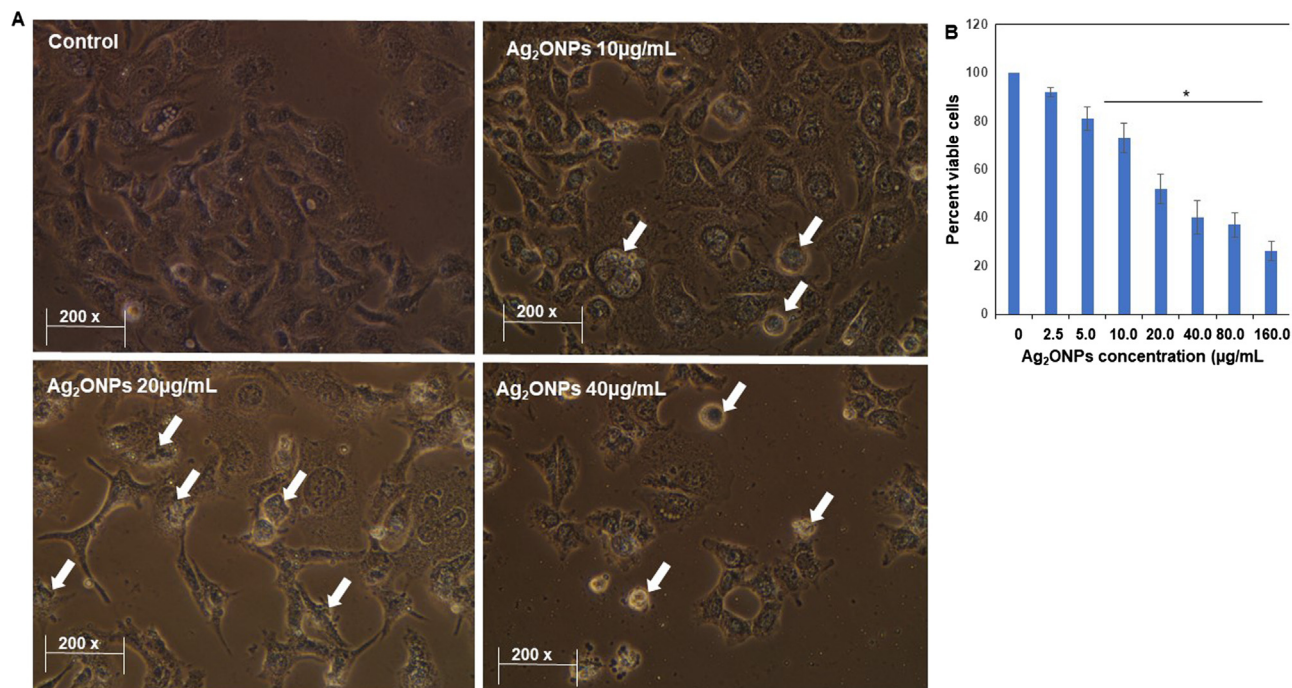


Fig. 7. Anticancer effect of Ag₂ONPs. Representative pictures of cells exposed with Ag₂ONPs for 24 h (A). Bar-diagram shows the viable cells after 24 h treatment of Ag₂ONPs (B). **P* ≤ 0.05 Vs Control, Values are mentioned as Mean ± S.D.

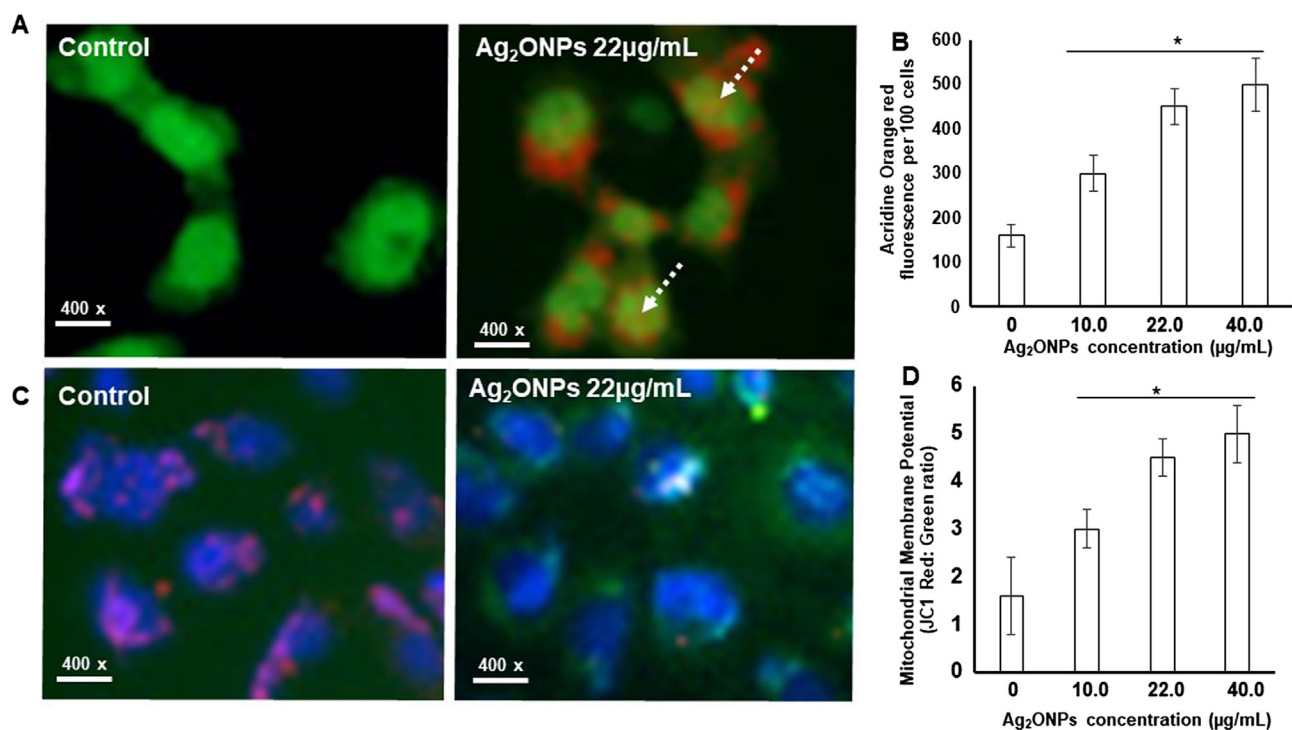


Fig. 8. Nuclear morphology, autophagy and MMP of normal and Ag₂ONPs treated cells. (A) Autophagy (AVO) was significantly observed (Dotted arrow) in control and different experimental conditions. (B) Red/green signal (arbitrary units) showing AVO positivity. (C) Fluorescence images of JC-1 and Hoechst stained Hep G2 cells. (D) The graph denotes the relative fluorescence unit of healthy (control) and treated Hep G2 cells. Data's were represented as mean ± S.D. * *P* < 0.05 Vs Control.

Table 1Antibacterial activity of Ag₂O NPs. The data's are mean ± standard deviation (mean ± SD; n = 3) Positive control- Ciprofloxacin (1 mg/mL), Negative control- DMSO (50 µL/well).

S1. No.	Ag ₂ O NPs or standard (µg/mL)	<i>Bacillus subtilis</i>	<i>Staphylococcus aureus</i>	<i>Escherichia coli</i>	<i>Pseudomonas aeruginosa</i>
1	2.5	3.16 ± 1.24	2.74 ± 0.98	1.98 ± 0.84	2.03 ± 0.65
2	5.0	5.24 ± 1.67	4.68 ± 1.29	3.49 ± 0.58	5.61 ± 1.06
3	10.0	11.89 ± 2.61	8.96 ± 2.36	6.76 ± 1.29	9.35 ± 1.54
4	20.0	19.43 ± 3.16	15.92 ± 2.68	13.62 ± 1.94	16.08 ± 2.04
5	40.0	22.26 ± 4.47	18.65 ± 3.15	16.33 ± 2.57	18.56 ± 1.57
6	Ciprofloxacin (1 mg/mL),	30.15 ± 1.62	28.09 ± 0.95	22.55 ± 1.15	23.15 ± 1.53

resonance could be attributed to the photodegradation activity of the Ag₂ONPs. Based on this remarkable photocatalytic activity it can be used for dye degradation efficiently. Present finding coincides with the reports of Lekshmi et al. (2022).

Hepatocellular carcinoma (HCC) is one among the most fatal diseases of cancer (Mir et al. 2021). The therapeutic option for HCC includes embolization, ablation, or both for the liver tumor (s). Additional choices may contain immunotherapy, targeted therapy, chemotherapy and/or radiation therapy (Mir et al. 2022). These treatment options are unlikely to cure the HCC patients. Researchers around the world are striving vigorously to formulate and announce innovative drug candidate with efficient therapeutic abilities. We have determined the anticancer potential of Ag₂ONPs (Fig. 7A-B). After 24 hrs treatment statistically significant ($P \leq 0.05$) reduction in cell survival was observed at 5 µg/mL of Ag₂ONPs treated cells. IC₅₀ was found to be 22 µg/mL. On further increase in Ag₂ONPs concentrations, cells, detach from the plate. Further we were interested to elucidate the possible mode of action of Ag₂ONPs induced cellular death. Autophagy experiment was analyzed using AO dye. In acid cubicles like lysosomes and autolysosomes, AO has protonated and emits red fluorescence due to aggregation. As shown in literature, numerous NPs induce anticancer effect by increasing the intracellular DNA damage and through autophagy (Hailan et al. 2022). In the present investigation we observed increased DNA damage level in HCC cells (Fig. 8A and B). We have also noticed a yellowish nucleus indicating nuclear damage (dotted arrow). This finding suggests that 22 µg/mL (IC₅₀) concentration of Ag₂ONPs induces considerable autophagy on cells by forming AVO. Often increased DNA damage decreases the MMP (Guo et al. 2022), which in turn induces cell death. In cellular toxicity, significant events occur in mitochondria; thus, the MMP is a fundamental analysis of the mitochondrial function that can be used as a sign of normal cell since mitochondria are inherently involved in the toxicity development of cells. Intact MMP is vital for cell proliferation (Tjahjono et al. 2022). In the present study we have noticed decreased MMP of Ag₂ONPs (Fig. 8C and D) treated cells. Decreased MMP correlate the increased cancer cell death.

It was visualized that dose of Ag₂ONPs were directly proportional to the antibacterial activities (Table 1). The observed antibacterial property of Ag₂ONPs is due to the occurrence of Ag⁺ ions, which inhibit and degrade the membrane proteins present in microbes. Further, in the current investigation Ag₂ONPs formed were spherical in nature, which are known to release more Ag⁺ ions due to their high surface area (Yin et al. 2020). The generation of reactive oxygen species (ROS) could be another reason for antibacterial effect of Ag₂ONPs. As ROS formed within the cells leads to cell death due to disparity in electron transport, interruption of energy transduction and/or cell lysis and decreased respiration (Slavin et al. 2017). The green Ag₂ONPs showed maximum antibacterial activity against gram-positive than that of gram-negative bacteria, with higher zone of inhibition. Ag₂ONPs shows great potency as effective source of drugs which easily reduces bacterial oriented diseases (Fayyadh and Alzubaidy, 2021). The results are also supported by Mollick et al. (2019).

4. Conclusions

The natural resource of phytochemicals occurring in the MeBEs of *D. montana* contributes to the efficient synthesis of Ag₂ONPs which are cost effective and easy to post harvest. SEM, TEM and XRD analysis confirmed its spherical shape Ag₂ONPs size ranging from ~ 6 nm to ~ 50 nm with face centered cubic phase crystalline in nature. The synthesized Ag₂ONPs were free of impurities and highly stable representing their enduring structure preservice. Ag₂ONPs displayed effective photocatalytic degradation indicating its active role as dye effluent. Significant antibacterial effect was exhibited by Ag₂ONPs against pathogenic microorganisms. *In vitro* anticancer studies clearly portrayed the pharmacological property of Ag₂ONPs against HCC which may contribute to its therapeutic potential. Thus, green synthesized Ag₂ONPs may play a vital role as dye effluent, antibacterial and anticancer agent demanding pre-clinical investigations to highlight its therapeutic efficacy.

Declaration of Competing Interest

The authors declare the following financial interests/personal relationships which may be considered as potential competing interests: [Sujatha V reports administrative support was provided by Pondicherry University. Sujatha V reports a relationship with Pondicherry University that includes: employment. Sujatha V has patent NIL pending to Not applicable. NIL].

Acknowledgements

The author VS acknowledges DST in the form of DST/KIRAN/Mobility/Sujatha/2019 (G) for the financial support rendered. STIC, Cochin University of Science and Technology, Cochin, India; CIF- Pondicherry University, Puducherry, India are acknowledged for the characterization studies.

Appendix A. Supplementary material

Supplementary data to this article can be found online at <https://doi.org/10.1016/j.jksus.2023.102563>.

References

- Ahmed, S., Ahmad, M., Swami, B.L., Ikram, S., 2016. A review on plants extract mediated synthesis of silver nanoparticles for antimicrobial applications: a green expertise. *J. Adv. Res.* 7, 17–28. <https://doi.org/10.1016/j.jare.2015.02.007>.
- Aisida, S.O., Ugwu, K., Nwanya, A.C., Bashir, A.K.H., Nwankwo, N.U., Ahmed, I., Ezema, F.I., 2021. Biosynthesis of silver oxide nanoparticles using leave extract of *Telfairia Occidentalis* and its antibacterial activity. *Mater. Today Proc.* 36, 208–213. <https://doi.org/10.1016/j.matpr.2020.03.005>.
- Aiswariya, K.S., Jose, V., 2022. Bioactive Molecules Coated silver oxide nanoparticle synthesis from *Curcuma zanthorrhiza* and HR-LCMS monitored validation of its photocatalytic potency towards malachite green degradation. *J. Clust. Sci.* 33, 1685–1696. <https://doi.org/10.1007/s10876-021-02099-0>.
- Ajitha, B., Reddy, Y.A.K., Reddy, P.S., 2015. Green synthesis and characterization of silver nanoparticles using Lantana camara leaf extract. *Mater. Sci. Eng. C. Mater. Biol. Appl.* 49, 373–381. <https://doi.org/10.1016/j.msec.2015.01.035>.

- Barreira, J.C.M., Ferreira, I.C.F.R., Oliveira, M.B.P.P., Pereira, J.A., 2008. Antioxidant activities of the extracts from chestnut flower, leaf, skins and fruit. *Food Chem.* 107, 1106–1113. <https://doi.org/10.1016/j.foodchem.2007.09.030>.
- Das, B., Dash, S.K., Mandal, D., Ghosh, T., Chattopadhyay, S., Tripathy, S., Das, S., Dey, S.K., Das, D., Roy, S., 2017. Green synthesized silver nanoparticles destroy multidrug resistant bacteria via reactive oxygen species mediated membrane damage. *Arab. J. Chem.* 10, 862–876. <https://doi.org/10.1016/j.arabj.2015.08.008>.
- Devanesan, S., AlSalhi, M.S., 2021. Green synthesis of silver nanoparticles using the flower extract of *Abelmoschus esculentus* for cytotoxicity and antimicrobial studies. *Int J Nanomed.* 14 (16), 3343–3356. <https://doi.org/10.2147/IJN.S307676>. PMID: 34017172.
- Dizge, N., Aydiner, C., Demirbas, E., Kobya, M., Kara, S., 2008. Adsorption of reactive dyes from aqueous solutions by fly ash: Kinetic and equilibrium studies. *J. Hazard. Mater.* 150, 737–746. <https://doi.org/10.1016/j.jhazmat.2007.05.027>.
- Erdogan, O., Abbak, M., Demirbolat, G.M., Birtekocak, F., Aksel, M., Pasa, S., Cevik, O., 2019. Green synthesis of silver nanoparticles via *Cynara scolymus* leaf extracts: The characterization, anticancer potential with photodynamic therapy in MCF7 cells. *PLoS One.* 14, e0216496.
- Fayyadh, A., Alzubaidy, J.M., 2021. Green-synthesis of Ag₂O nanoparticles for antimicrobial assays. *J. Mech. Behav. Mater.* 30, 228–236. <https://doi.org/10.1515/jmbm-2021-0024>.
- Guo, Y., Jin, S., Song, D., Yang, T., Hu, J., Hu, X., Han, Q., Zhao, J., Guo, Z., Wang, X., 2022. Amlexanox-modified platinum (IV) complex triggers apoptotic and autophagic bimodal death of cancer cells. *Eur. J. Med. Chem.* 15, 114691. <https://doi.org/10.1016/j.ejmech.2022.114691>.
- Hailan, W.A., Al-Anazi, K.M., Farah, M.A., Ali, M.A., Al-Kawmani, A.A., Abou-Tarboosh, F.M., 2022. Reactive oxygen species-mediated cytotoxicity in liver carcinoma cells induced by silver nanoparticles biosynthesized using *Schinus mole* extract. *Nanomaterials* 12, 161. <https://doi.org/10.3390/nano12010161>.
- Kadmir, J., Dhawal, P., Barve, S., Kakodkar, S., 2020. Green synthesis of silver nanoparticles using cauliflower waste and their multifaceted applications in photocatalytic degradation of methylene blue dye and Hg²⁺ biosensing. *SN Appl. Sci.* 2, 738. <https://doi.org/10.1007/s42452-020-2543-4>.
- Kale, R.D., Kane, P., 2017. Colour removal using nanoparticles. *Text. Cloth. Sustain.* 2, 4. <https://doi.org/10.1186/s40689-016-0015-4>.
- Kathirvel, A., Sujatha, V., 2016. Phytochemical studies, antioxidant activities and identification of active compounds using GC–MS of *Dryopteris cochleata* leaves. *Arab. J. Chem.* 9, S1435–S1442. <https://doi.org/10.1016/j.arabj.2012.03.018>.
- Khan, M.T., Azhar, I., Shehzadi, N., Hussain, K., Parveen, S., Hanif, U., 2020. Morphological, microscopic, and physicochemical studies of *Diospyros montana*. *Microsc. Res. Tech.* 83, 1260–1281. <https://doi.org/10.1016/j.phyplu.2021.100150>.
- Kokila, K., Elavarasan, N., Sujatha, V., 2017. *Diospyros montana* leaf extract-mediated synthesis of selenium nanoparticles and their biological applications. *New J. Chem.* 41, 7481–7490. <https://doi.org/10.1039/C7NJ01124E>.
- Lekshmi, G.S., Tamilselvi, R., Geethalakshmi, R., Kirupha, S.D., Bazaka, O., Levchenko, I., Mandhakini, M., 2022. Multifunctional oil-produced reduced graphene oxide–silver oxide composites with photocatalytic, antioxidant, and antibacterial activities. *J. Colloid Interface Sci.* 608, 294–305. <https://doi.org/10.1016/j.jcis.2021.08.048>.
- Maheshwaran, G., Nivedhitha Bharathi, A., Malai Selvi, M., Krishna Kumar, M., Mohan Kumar, R., Sudhahar, S., 2020. Green synthesis of Silver oxide nanoparticles using *Zephyranthes rosea* flower extract and evaluation of biological activities. *J. Environ. Chem. Eng.* 8. <https://doi.org/10.1016/j.jece.2020.104137> 104137.
- Manikandan, V., Velmurugan, P., Park, J.H., Chang, W.S., Park, Y.J., Jayanthi, P., Oh, B. T., 2017. Green synthesis of silver oxide nanoparticles and its antibacterial activity against dental pathogens. *Biotech.* 7, 72. <https://doi.org/10.1007/s13205-017-0670-4>.
- Mao, Y., Park, T.J., Wong, S.S., 2005. Synthesis of classes of ternary metal oxide nanostructures. *Chem. Commun.* 46, 5721–5735. <https://doi.org/10.1039/B509960A>.
- Mathew, S., Abraham, T.E., Zakaria, Z.A., 2015. Reactivity of phenolic compounds towards free radicals under *in vitro* conditions. *J. Food Sci. Technol.* 52, 5790–5798. <https://doi.org/10.1007/s13197-014-1704-0>.
- Mir, I.H., Guha, S., Behera, J., Thirunavukkarasu, C., 2021. Targeting molecular signal transduction pathways in hepatocellular carcinoma and its implications for cancer therapy. *Cell Biol. Int.* 45, 2161–2177. <https://doi.org/10.1002/cbin.11670>.
- Mir, I.H., Jyothi, K.C., Thirunavukkarasu, C., 2022. The prominence of potential biomarkers in the diagnosis and management of hepatocellular carcinoma: current scenario and future anticipation. *J. Cell Biochem.* 123, 1607–1623. <https://doi.org/10.1002/jcb.30190>.
- Mollick, M.M.R., Rana, D., Dash, S.K., Chattopadhyay, S., Bhowmick, B., Maity, D., Mondal, D., Pattanayak, S., Roy, S., Chakraborty, M., Chattopadhyay, D., 2019. Studies on green synthesized silver nanoparticles using *Abelmoschus esculentus* (L.) pulp extract having anticancer (*in vitro*) and antimicrobial applications. *Arab. J. Chem.* 12, 2572–2584. <https://doi.org/10.1016/j.arabj.2015.04.033>.
- Okafor, F., Janen, A., Kukhtareva, T., Edwards, V., Curley, M., 2013. Green synthesis of silver nanoparticles, their characterization, application and antibacterial activity. *Int. J. Environ. Res. Public Health.* 10, 5221–5238. <https://doi.org/10.3390/ijerph10105221>.
- Onwukeame, D.M., Ikuegbvweha, T.B., Asonye, C.C., 2007. Evaluation of phytochemical constituents, antibacterial activities and effect of exudate of *Pycnanthus Angolensis* Wedl Warb (Myristicaceae) on corneal ulcers in rabbits. *Trop. J. Pharm. Res.* 6 (2), 725–730. <https://doi.org/10.1126/science.179.4073.588>.
- Palanisamy, S., Rajasekar, P., Vijayaprasath, G., Ravi, G., Manikandan, R., Prabhu, N. M., 2017. A green route to synthesis silver nanoparticles using *Sargassum polycystum* and its antioxidant and cytotoxic effects: an *in vitro* analysis. *Mater. Lett.* 189, 196–200. <https://doi.org/10.1016/j.matlet.2016.12.005>.
- Perelman, A., Wachtel, C., Cohen, M., Haupt, S., Shapiro, H., Tzur, A., 2012. JC-1: Alternative excitation wavelengths facilitate mitochondrial membrane potential cytometry. *Cell Death Dis.* 3, e430.
- Raja, P.B., Rahim, A.A., Qureshi, A.K., Awang, K., 2014. Green synthesis of silver nanoparticles using tannins. *Mater. sci. pol.* 32, 408–413. <https://doi.org/10.2478/s13536-014-0204-2>.
- Roy, K., Sarkar, C.K., Ghosh, C.K., 2015. Plant-mediated synthesis of silver nanoparticles using parsley (*Petroselinum crispum*) leaf extract: spectral analysis of the particles and antibacterial study. *Appl. Nanosci.* 5, 945–951. <https://doi.org/10.1007/s13204-014-0393-3>.
- Sadeghi, B., Gholamhoseinpoor, F., 2015. A study on the stability and green synthesis of silver nanoparticles using *Ziziphora tenuior* (Zt) extract at room temperature. *Spectrochim. Acta. A Mol. Biomol. Spectrosc.* 134, 310–315. <https://doi.org/10.1016/j.saa.2014.06.046>.
- Singh, J., Dutta, T., Kim, K.H., Rawat, M., Samddar, P., Kumar, P., 2018. 'Green' synthesis of metals and their oxide nanoparticles: applications for environmental remediation. *J. Nanobiotechnol.* 16, 84. <https://doi.org/10.1186/s12951-018-0408-4>.
- Slavin, Y.N., Asnis, J., Häfeli, U.O., Bach, H., 2017. Metal nanoparticles: understanding the mechanisms behind antibacterial activity. *J. Nanobiotechnology.* 15, 65. <https://doi.org/10.1186/s12951-017-0308-z>.
- Srinivasan, R., Natarajan, D., Shivakumar, M.S., 2016. *In vitro* evaluation of antioxidant, antiproliferative potentials of bioactive extract-cum-rutin compound isolated from *Memecylon edule* leaves and its molecular docking study. *J. Biologi. Acti. Produ. Nat.* 6, 43–58. <https://doi.org/10.1080/22311866.2016.1173592>.
- Subastri, A., Suyavaran, A., Preedia Babu, E., Nithyananthan, S., Barathidasan, R., Thirunavukkarasu, C., 2018. Troxerutin with copper generates oxidative stress in cancer cells: its possible chemotherapeutic mechanism against hepatocellular carcinoma. *J. Cell Physiol.* 233, 1775–1790. <https://doi.org/10.1002/jcp.26061>.
- Sujatha, V., Venkatesan, A., 2022. Brief review of the genus *Diospyros Montana* Roxb: Phytochemical properties. *Exstsv. Rev.* 2, 11–19. <https://doi.org/10.21467/exr.2.1.4572>.
- Thomé, M.P., Filippi-Chiela, E.C., Villodre, E.S., Migliavaca, C.B., Onzi, G.R., Felipe, K. B., Lenz, G., 2016. Radiometric analysis of Acridine Orange staining in the study of acidic organelles and autophagy. *J. Cell Sci.* 129, 4622–4632. <https://doi.org/10.1242/jcs.195057>.
- Tjahjono, E., Kirienko, D.R., Kirienko, N.V., 2022. The emergent role of mitochondrial surveillance in cellular health. *Aging Cell.* 00, e13710. <https://doi.org/10.1111/ace1.13710>.
- Velsankar, K., Parvathy, G., Sankaranarayanan, K., Mohandoss, S., Sudhahar, S., 2022. Green synthesis of silver oxide nanoparticles using *Panicum milaceum* grains extract for biological applications. *Adv. Powder Technol.* 33. <https://doi.org/10.1016/j.apt.2022.103645> 103645.
- Wei, S., Wang, Y., Tang, Z., Hu, J., Su, R., Lin, J., Zhou, T., Guo, H., Wang, N., Xu, R., 2020. A size-controlled green synthesis of silver nanoparticles by using the berry extract of Sea Buckthorn and their biological activities. *New J. Chem.* 44, 9304–9312. <https://doi.org/10.1039/D0NJ01335H>.
- Yin, I.X., Zhang, J., Zhao, I.S., Mei, M.L., Li, Q., Chu, C.H., 2020. The antibacterial mechanism of silver nanoparticles and its application in dentistry. *Int. J. Nanomedicine.* 15, 2555–2562. <https://doi.org/10.2147/IJN.S246764>.